THE JOURNAL OF PHYSICAL CHEMISTRY B

Article

pubs.acs.org/JPCB

Influence of Backbone Rigidness on Single Chain Conformation of Thiophene-Based Conjugated Polymers

Zhongjian Hu,[†] Jianhua Liu,[‡] Lauren Simón-Bower, Lei Zhai,* and Andre J. Gesquiere*

NanoScience Technology Center, Department of Chemistry and CREOL, The College of Optics and Photonics, 12424 Research Parkway Suite 400, University of Central Florida, Orlando, Florida 32826, United States

ABSTRACT: Structural order of conjugated polymers at different length scales directs the optoelectronic properties of the corresponding materials; thus it is of critical importance to understand and control conjugated polymer morphology for successful application of these materials in organic optoelectronics. Herein, with the aim of probing the dependence of single chain folding properties on the chemical structure and rigidness of the polymer backbones, single molecule fluorescence spectroscopy was applied to four thiophene-based conjugated polymers. These include regioregular poly(3-hexylthiophene) (RR-P3HT), poly-(2,5-bis(3-tetradecylthiophen-2-yl)thieno[3,2-*b*]thiophene) (PBTTT-14), poly(2,5-bis(3-tetradecylthiophen-2-yl)thiophene-2-yl)thiophen-2-ylthiazolo[5,4-*d*]thiazole) (PTzQT-12), and poly(3,3-didodecylquaterthiophene)] (PQT-12). Our previous work has shown that RR-P3HT and PBTTT-14 polymer chains fold in their nanostructures, whereas PQT-12 and PTzQT-12 do not fold in their nanostructures. At the single molecule level, it was found that RR-P3HT single chains almost exclusively fold into loosely and strongly aggregated conformations, analogous to the folding properties in nanostructures. PQT-12 displays significant chain folding as well, but only into loosely aggregated conformations, showing an absence of strongly aggregated polymer chains. PBTTT-14 exhibits a significant fraction of rigid polymer chain. The findings made for single molecules of PQT-12 and PBTTT-14 are thus in contrast with the observations made in their corresponding nanostructures. PTzQT-12 appears to be the most rigid and planar conjugated polymer of these four polymers. However, although the presumably nonfolding polymers PQT-12 and PTzQT-12 exhibit less folding than RR-P3HT, there is still a significant occurrence of chain folding for these polymers at the single molecule level. These results suggest that the folding properties of conjugated polymers can be influenced by the architecture of the polymer backbones; however, other factors such as intermolecular stacking interactions, solvent environment, and side chain interactions in corresponding materials should also be taken into account to predict conjugated polymer material morphology.

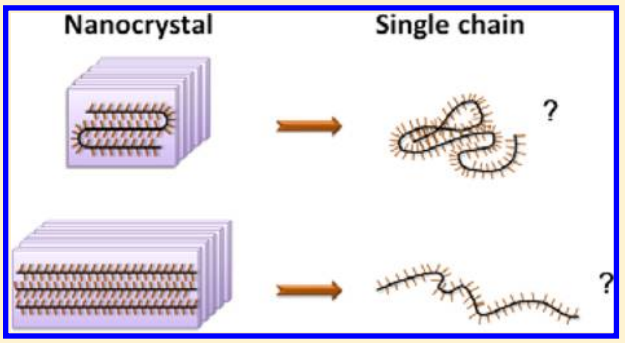

1. INTRODUCTION

In conjugated polymer based organic opto-electronic devices such as organic field effect transistors (OFETs) and organic photovoltaics (OPVs), the polymer chains form ordered structures from the nano- to macroscale that are of critical importance in determining device properties, function, and performance.[1,2] These ordered structures exhibit an intimate contact between adjacent conjugated polymer backbones that facilities efficient and rapid migration of excitations and charges through the conjugated polymer material. Investigations on the aggregation and crystallization behavior of conjugated polymers are therefore imperative for studying intrinsic exciton and charge transport properties, understanding the fundamental structure−property relations and designing novel polymers with optimized properties. The aggregation and crystallization behavior at different length scales is expected to largely depend on the chemical structure (architecture) and morphology of the individual chains.[1,3−5]

Thiophene-based conjugated polymers, which show meso-scale crystallization behavior, have been intensively studied in organic opto-electronic devices over the past decade due to their desirable properties, such as the ability to self-organize into highly ordered structures that facilitate high charge mobility and a broad absorbing range of visible light.[6] With scanning tunneling microscopy (STM), researchers have been able to directly visualize chain folding (i.e., a polymer chain folds, i.e., collapses, at a defect such as a missing double bond or rotates around a single bond- into a two- or three-dimensional structure starting from random coil or extended chain) for a few different conjugated polymers of this class. These studies have revealed a significant chain folding in two-dimensional poly (3-alkylthiophene) (P3AT) layers,[3,4] whereas extended (nonfolded) chains were detected for the conjugated polymer poly[(5,5′-(3,3′-di-*n*-octyl-2,2′-bithiophene))-*alt*-(2,7-fluoren-9-one)] (PDOBT). The latter polymer has a more rigid backbone.[4] These molecular structure-dependent folding

Special Issue: Paul F. Barbara Memorial Issue

Received: August 27, 2012
Revised: December 10, 2012
Published: December 20, 2012

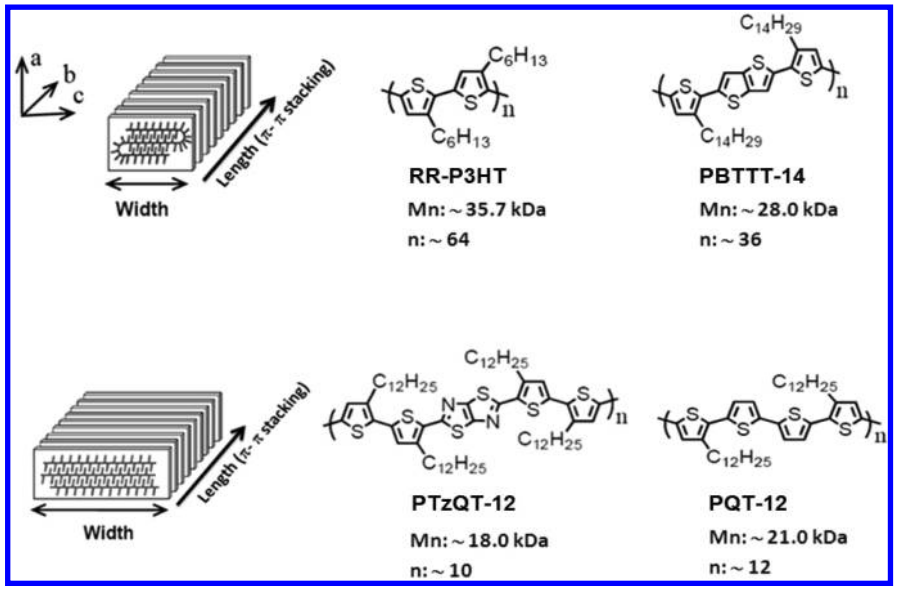

Figure 1. Illustrations of nanostructure morphologies with polymer chain folding (top left) and nonfolding chains (bottom left). RR-P3HT and PBTTT-14 polymer chains exhibit folding and PTzQT-12 and PQT-12 show nonfolding behavior in their nanocrystals.[8] Beneath the chemical structure of each polymer, the number average molecule weight (M_n) and the number of repeat units are given. Note that the numbers of repeat units were calculated from corrected values of M_n because GPC tends to overestimate the actual molecular weight of rigid-rod conjugated polymers by a factor of about 1.7.[32] The PDIs of these four polymers are in the range of 1.5−1.7.

properties are expected to dominate the aggregation and crystallization behaviors in three dimensions into fibrillar or ribbon-like structures.

Recently, by characterizing self-assembled nanostructures formed by polythiophene and its derivatives in dilute solutions using marginal solvents, the chain folding properties of four different thiophene-based polymers, shown in Figure 1, were investigated. Crystalline strcutures with distinct folding and nonfolding properties of these polymers as a function of backbone architecture were observed.[7,8] Briefly, with similar number average molecule weight, the conjugated polymers regioregular poly (3-hexylthiophene) (RR-P3HT) and poly-(2,5-bis(3-tetradecylthiophen-2-yl)thieno[3,2-*b*]thiophene) (PBTTT-14) show polymer chain folding in the corresponding nanocrystals whereas poly(2,5-bis(3-tetradecylthiophen-2-yl)-thiophene-2-yl)thiophen-2-ylthiazolo[5,4-*d*]thiazole) (PTzQT-12), and poly(3,3-didodecyl-quaterthiophene)] (PQT-12) exhibit no folding of the polymer chains; i.e., PQT-12 and PTzQT-12 are nonfolding polymers in their self-assembled crystalline structures. This experimental finding was corroborated by a computational analysis with respect to the rotation energy barrier of inter-ring σ bonds along the polymer backbone.[8] Although a relationship between the backbone stiffness and macroscopic crystallization behavior has been interrogated, it is not clear (i) whether this kind of folding or nonfolding conformation occurs at the single molecular level (i.e., property of individual chains) or in a specific crystallization environment (i.e., property of the crystal), and (ii) what are the possible different conformations at the single molecule level.

Single molecule spectroscopy (SMS) has been proven to be a powerful tool in probing the photophysics, photochemistry and conformation of individual chains of conjugated polymers.[9−13] Herein, we extend SMS studies to the investigation of the morphological properties of individual polymer chain of these four different thiophene-based conjugated polymers with the aim of understanding the correlation between the polymer folding properties and polymer backbone rigidness at the single chain level. Our results indicate that the folding and nonfolding behavior of the polymers under investigation is strongly but not uniquely related to the backbone rigidness of the polymers. Although in nanoscale (poly)crystalline materials RR-P3HT and PBTTT-14 show folding and PQT-12 and PTzQT-12 are nonfolding polymers in these experiments, the SMS data presented here indicate that PQT-12 and PTzQT-12 still show a significant fraction of folded chains at the single molecule level. Furthermore, different degrees and fractions of chain folding are observed as a function of polymer backbone architecture. The comparison of studies of polymer chain conformation in materials such as nanowires and nanoribbons and single chain studies shows that the polymer chain folding properties of conjugated polymer molecules are dominated not only by backbone architecture (typically aimed at increasing chain rigidness) but also by other factors such as interchain interactions and side chain characteristics, which should be considered.

2. EXPERIMENTAL SECTION

RR-P3HT and poly(methyl methacrylate) (PMMA) were bought from Rieke Metals. PQT-12 was purchased from American Dye Source, Inc. PBTTT-14 (lisiconSP210) and PTzQT-12 were provided by Merck Chemicals, Ltd. and Dr. Richard D. McCullough's group. The molecular weight and polydispersity index (PDI) of the polymers are given in Figure 1. The suspended nanocrystals of conjugated polymers were prepared in dilution solutions (0.1−0.2 mg/mL) of their suitable marginal solvents as previously reported.[8] The morphology of the prepared crystals was characterized by transmission electron microscopy (TEM, JEOL 1011) at 100 kV. SMS samples were prepared by spin coating a 2 wt % PMMA solution in chloroform (OmniSolv, 99.8%, EMD) containing an appropriate concentration of conjugated polymers onto a clean cover slide followed by thermal deposition of a ~200 nm thick aluminum film to prevent

dx.doi.org/10.1021/jp308497k | J. Phys. Chem. B 2013, 117, 4461−4467

photobleaching during the experiments. The single conjugated polymer chain in PMMA can be closely representative of its equilibrium conformations as Vogelsang demonstrated previously.[14,15] The SMS experimental apparatus is a home-built sample scanning confocal microscope that has been described elsewhere.[10] In addition to single molecule spectroscopy, a single molecule fluorescence emission polarization experiment was also carried out with the same confocal microscope to further understand the conformation of single molecules. Circularly polarized excitation laser light was used and the fluorescence signal was split into two orthogonal directions by a broad-band polarizing cube beam splitter (Newport, 05FC16PB.3) and detected with two avalanche photodiodes (Perkin-Elmer SPCM-AQR-14). The correction factor for this setup was determined to be 0.79 using a TransFluoSpheres bead sample (carboxylate-modified microspheres, 0.1 μm, 488/560, Invitrogen) at 488 nm excitation. Reported polarization ratios (P) were calculated using image analysis software home-written in MatLab.

3. RESULTS AND DISCUSSION

3.1. Crystallization Behavior. Figure 2 shows representative TEM images of solution prepared nanostructures of the polymers interrogated in present work. As can be seen, the nanostructures display distinct morphologies for different polymers. RR-P3HT and PBTTT-14 nanostructures show very high aspect ratio with the nanowire width much smaller than the contour length of the constituent conjugated polymers. In contrast, the nanostructures of PQT-12 and PTzQT-12 exhibit a lower aspect ratio and a nanowire width comparable to the contour length of the constituent conjugated polymers. The nanofibrillar structure width measured with TEM and the contour length calculated on the basis of M_n are displayed in Table 1. Previous theoretical calculations by Mena-Osteritz[3] have indicated that the folded region of a polymer chain requires a consecutive syn conformation of thiophene rings whereas an extended polymer chain prefers an anti conformation. Therefore, the rotation energy barrier of inter-ring σ bond along the polymer backbone, projected by the tendency of transformation between anti and syn conformations, should be strongly related to the polymer chain folding behavior. A thorough theoretical analysis concerning the rotation energy barrier of inter-ring σ bond of the four polymers investigated here has been reported in detail previously and supports the experimental observations made for the polymer chain conformations in the nanostrucutres.[8]

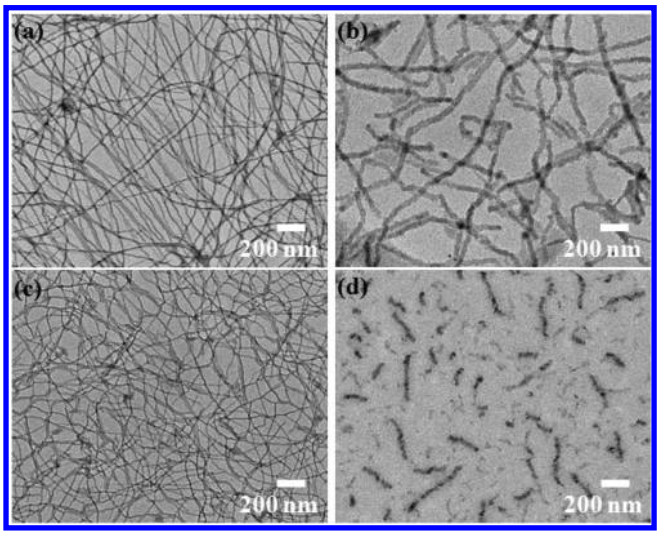

Figure 2. TEM images of solution prepared nanocrystals of (a) RR-P3HT, (b) PQT-12, (c) PBTTT-14, and (d) PTzQT-12, respectively.

3.2. Molecular Solution Spectroscopy. Figure 3 summarizes the absorption and emission spectra of chloroform solutions of RR-P3HT, PQT-12, PBTTT-14, and PTzQT-12. Although RR-P3HT and PQT-12 have an analogous thiophene backbone architecture, the absorption maximum of PQT-12 (Figure 3b) is red-shifted to 477 nm compared with 452 nm for RR-P3HT (Figure 3a), due to chromophores with a longer conjugation length (i.e., delocalization of electrons in π-bonds, which reduces the observed band gap and is favored by more coplanar aromatic rings and disfavored by torsion (twist or rotation), kink (sharp turn in backbone propagation at defect), or bend (due to rotation around consecutive single bonds, e.g., observed for P3HT with STM, vide supra) in the backbone) presumably resulting from a more planar backbone of PQT-12. The absorption spectrum of PBTTT-14 (Figure 3c) exhibits a 22 nm red shift relative to RR-P3HT, due to a rigid backbone caused by the fused thiophene ring and the presence of the highly delocalized thienothiophene aromatic rings in PBTTT-14.[2,16,17] The appearance of a shoulder at ~590 nm in the absorption spectrum is probably caused by intrachain $\pi-\pi$ association.[18] The absorption spectrum of PTzQT-12 in Figure 3d peaks at 545 nm and exhibits two pronounced vibronic features at ~590 nm (with stronger intensity than observed for PBTTT-14) and 640 nm. The energy differences of about 0.17 eV between the absorption maximum and shoulder and between shoulder and shoulder can be associated to the C=C stretching vibration of the thiophene ring, which has an energy of 0.18 eV.[19,20] The red-shifted maximum and structured vibronic features of PTzQT-12 absorption spectrum compared with the other three polymers are attributed to a very rigid and coplanar backbone, and an enhanced intramolecular charge transfer in the donor–acceptor type backbone due to

Table 1. Summary of Polymer Chain Folding Properties of Nanocrystals (from TEM Imaging) and at the Single Chain Level Based on SMS Analysis of the Four Polymers Studied in the Present Work

polymers		RR-P3HT	PQT-12	PBTTT-14	PTzQT-12
mol wt (M_n, kDa)		35.7	21	28	18
nanocrystal	nanowire width (nm)	15	31	14	21
	contour length (nm)	48	29	32	18
	chain conformation	folding	nonfolding	folding	nonfolding
single chain conformation (by SMS)	extended	8%	33%	54%	65%
	loosely aggregated	58%	67%	21%	18%
	strongly aggregated	34%		25%	17%

dx.doi.org/10.1021/jp308497k | J. Phys. Chem. B 2013, 117, 4461–4467

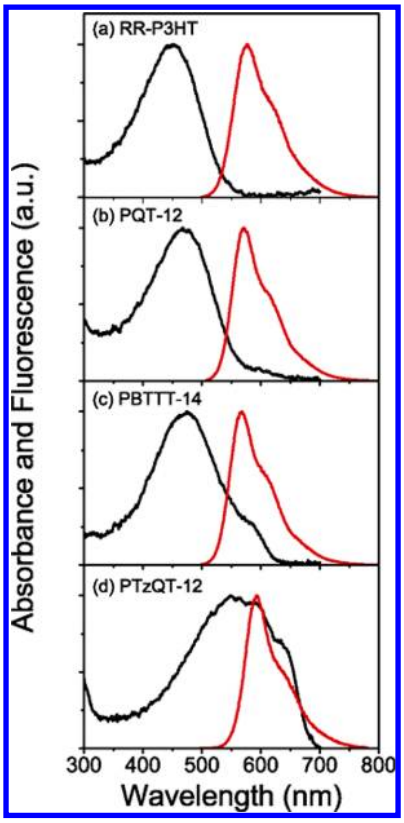

Figure 3. Absorption (black) and fluorescence emission spectra (red) of chloroform solutions of (a) RR-P3HT, (b) PQT-12, (c) PBTTT-14, and (d) PTzQT-12, respectively.

the introduction of thiazolothiazole unit.[21,22] Compared with the Stokes shift value of 125 nm for RR-P3HT, the values of Stokes shift for PQT-12, PBTTT-14 and PTzQT-12 are 104, 94, and 43 nm, respectively. These reduced Stokes shift values for PQT-12, PBTTT-14, and PTzQT-12 can be attributed to reduced degrees of freedom and conformational reorganization in the excited state as a result of polymer backbone rigidity.[23,24]

3.3. Single Molecule Spectroscopy. *RR-P3HT.* As shown in Figure 4a-1 for the RR-P3HT, a strong red shift in the emission of ~43 nm can be observed in single molecule ensemble spectra with respect to the corresponding molecular chloroform solution. Similar results also have been observed for poly(3-octylthiophene) with a molecule weight of 143 kDa and have been ascribed to the planarization of the polymer backbone and the dominant occurrence of low energy site emission of aggregated conformations in the solid state.[12] These low energy sites are believed to be due to conjugated chain contacts or longer conjugated segments in a collapsed chain conformation, which causes a local lowering of the exciton energy.[9,25,26] As reported in previous work, the broad peak wavelength distribution of RR-P3HT and P3OT actually represents a bimodal distribution of peak wavelengths that is masked by the greater energy disorder in the chromophores[10,12] compared to, for instance, MEH-PPV.[25,26] Data in this paper were treated according to methods used in those reports, and in most cases the distribution was apparent, presumably due to the lower molecular weight of the polymers that were studied. From the peak wavelength distribution histogram shown in Figure 4a-2, it can be seen that a small fraction of molecules (marked with green) are still peaked at ~577 nm (peak wavelength of molecular solution). The

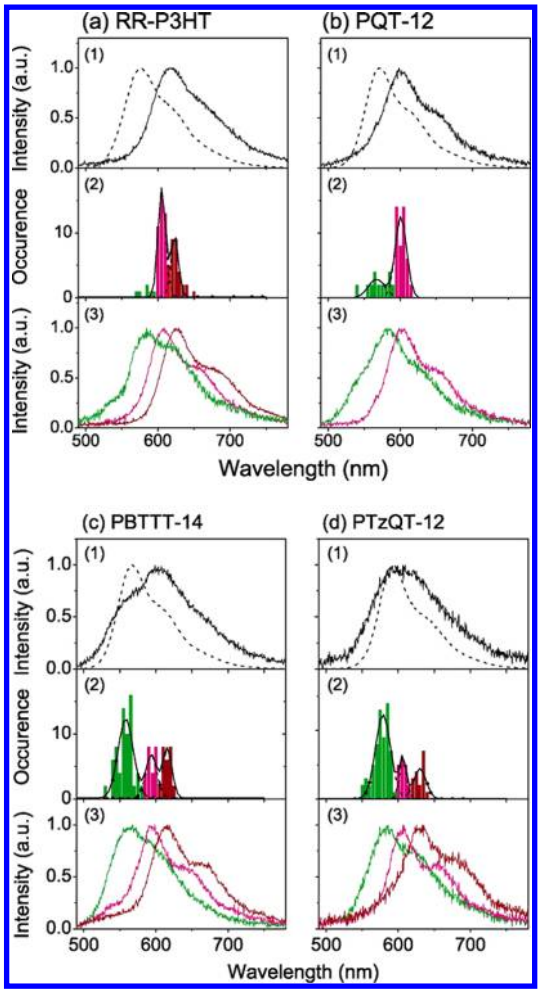

Figure 4. Single molecule spectral data for (a) RR-P3HT, (b) PQT-12, (c) PBTTT-14, and (d) PTzQT-12. For each polymer, the normalized single molecule ensemble spectrum (solid curve) and the solution emission (dashed curve) are depicted in the top panels (panel a-1, b-1, c-1 and d-1). The middle panels (panel a-2, b-2, c-2, and d-2) demonstrate the peak wavelength distribution histograms that are fitted to Gaussians (black curves). The bottom panels (panel a-3, b-3, c-3, and d-3) display the normalized subensemble spectra created according to the color scheme indicated in the corresponding peak wavelength distribution histograms (based on the Gaussian fitting).

somewhat unexpected presence of molecules with solution-like emission spectra might be a result from a random and rapid "freezing" of molecular conformation from solution into PMMA film during the spin coating process and may also indicate the presence of low molecular weight species with decreased conjugation length. For the RR-P3HT studied in the present work, more chain packing would be expected, therefore leading to a higher occurrence of lower energy site emission because of intramolecular energy transfer. As shown in Figure 4a-2, a bimodal distribution of peak emission wavelengths corresponding to solution-like (green) and loosely aggregated (magenta) chains can be observed, similar to the case for low molecular weight RR-P3HT investigated before.[10] However, the occurrence of molecules with solution-like conformations has significantly decreased compared to that for low molecular weight RR-P3HT. In addition, a third peak in the histogram (red) assigned to emission from polymer chains with a strongly aggregated conformation can be observed. The subensemble spectra for RR-P3HT shown in Figure 4a-3 are constructed by

dx.doi.org/10.1021/jp308497k | J. Phys. Chem. B 2013, 117, 4461−4467

averaging the single molecule spectra with peak wavelengths indicated by the different colors in the corresponding peak wavelength histograms in Figure 4a-2. For the red and magenta subensemble spectra of RR-P3HT, we can see that the 0−1 electronic transition intensity distinctly decreases in comparison with the green (solution-like) subensembles of RR-P3HT. The Huang−Rhys factor **S**, a measure of the electron-vibration coupling between the ground and excited states, associated with the *n*th active mode, in the case of a single emitting species **S** can be empirically estimated from the ratio of fluorescence intensity of the 0−1 transition to that of the 0−0 transition, i.e., $\mathbf{S} = I_{0-1}/I_{0-0}$.[25] Previous investigations indicate that **S** has been correlated with the conformational disorder of polymer chains and exciton migration in bulk materials, for which smaller **S** indicates a longer conjugation length and a larger extent of exciton migration in the conducting polymers.[25,27] It can be clearly seen that, for RR-P3HT single molecules, the **S** value decreases for the red and magenta subensemble compared with the green subensemble, indicative of a more effective exciton migration and longer conjugation length, i.e., a collapsed and ordered structure (chain folding). The highly ordered aggregated conformation of RR-P3HT single molecules can be substantiated by the high polarization ratio (P) values with maximum around 0.75 in the P distribution histogram of statistical ensemble of the polymer molecules as shown in Figure 5a. Recent work by Adachi et al., using fluorescence

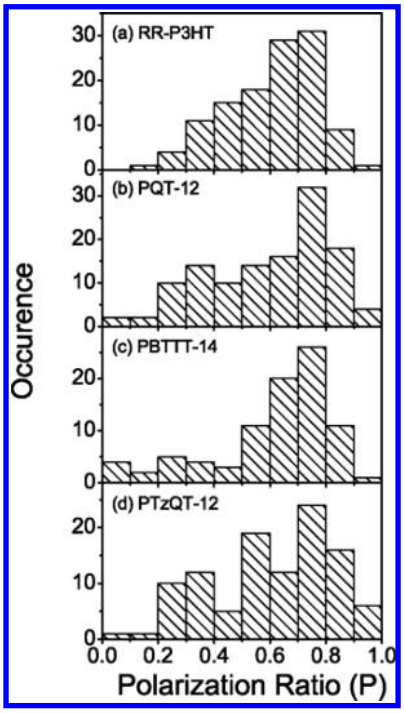

Figure 5. Polarization ratio (P) distribution histograms for (a) RR-P3HT, (b) PQT-12, (c) PBTTT-14, and (d) PTzQT-12, respectively.

excitation polarization spectroscopy, has also revealed similar RR-P3HT folding into highly ordered aggregates corresponding to what is observed herein.[28] Occurrences near moderate polarization ratio range might result from the contributions of more disordered molecules exhibiting solution-like spectra and/or the random orientation of the molecules with respect to the lab frame.

PQT-12. Although PQT-12 and RR-P3HT have analogous thiophene backbone structures and solution fluorescence spectra, these two polymers exhibit dissimilar single molecule emission features. As shown in Figure 4a-1 and 4b-1, the peak emission wavelength of the RR-P3HT SMS ensemble spectrum is 25 nm red-shifted relative to that of the PQT-12 ensemble spectrum. In comparison with the bimodal distribution of peak wavelengths of RR-P3HT over the wavelength range 597−650 nm (Figure 4a-2), there is only a narrow single modal distribution of peak emission wavelengths from 593 to 615 nm in PQT-12 data (Figure 4b-2). This observation can be explained by a possible inhibition of forming a strongly aggregated conformation by PQT-12 chains. Additionally, from the peak wavelength distribution histogram of PQT-12, one can see that ∼33% of single molecules assume solution-like conformations. This reduction of the occurrence of folded molecules when PQT-12 is compared with RR-P3HT can be explained by a higher rotation energy barrier of inter-ring σ-bond proposed previously.[8] From the P distribution histogram in Figure 5b, it can be found that the majority of PQT-12 molecules exhibit high P value, analogous to P3HT molecules, suggesting the loosely aggregated conformation of PQT-12 is also highly ordered.

PBTTT-14. Figure 4c-1 presents SMS ensemble spectra for PBTTT-14. The molecular solution fluorescence spectrum is included as a black dashed curve for comparison. As can be seen for PBTTT-14, the peak wavelength of the single molecule ensemble spectrum is red-shifted to 605 nm with a pronounced shoulder at 560 nm. The corresponding peak wavelength distribution histogram (Figure 4c-2) exhibits a maximum at 565 nm, which is close to the molecular solution emission maximum at 568 nm, as well as a broad red-shifted distribution above 583 nm. These data indicate that the single molecule ensemble spectrum of PBTTT-14 is formed by the contribution from solution-like and aggregated polymer chains. This finding is evident from the subensemble spectra displayed in Figure 4c-3 that were constructed according to the peak wavelength distribution histogram in Figure 4c-2. Again, the green subensemble spectrum is very similar to the solution fluorescence spectrum. Due to a more rigid backbone in PBTTT-14 as a result of a fused thiophene ring, the PBTTT-14 molecule has less conformational freedom compared to RR-P3HT molecules.[108,109] This explains the strong presence of the green subensemble showing molecular solution-like emission characteristics in the SMS data (about half of the population). The appearance of red-shifted emission from PBTTT-14 single molecules indicates collapsed conformations for these particular PBTTT-14 single molecules (∼46% in this case) in the SMS samples. The distribution within the long wavelength range (583−630 nm) can be fitted to two Gaussian curves (Figure 4c-2). This bimodal distribution resembles that found in RR-P3HT molecules and can be described as loosely and strongly aggregated conformations. Similar to the other polymers, the subensemble spectra built from the subpopulations of aggregated chains exhibit a markedly well-defined vibronic structure in which the ratio of fluorescence intensity of the 0−1 transition to that of the 0−0 transition is significantly smaller compared to molecular solution data. The latter observation is analogous to that found for RR-P3HT, indicating a more effective exciton migration and longer conjugation length, i.e., a collapsed and ordered structure (chain folding). The appearance of defined vibronic structure for the magenta and red subensemble spectra is indicative of emission occurring from a limited number of emitters on the chains, again indicating exciton migration to low energy trap sites.[26]

dx.doi.org/10.1021/jp308497k | J. Phys. Chem. B 2013, 117, 4461−4467

The P distribution histogram of PBTTT-14 displays a low occurrence of P values below 0.5 and a large number of occurrences above 0.6 (Figure 5c). However, the high polarization ratios are surprising when a 54% occurrence of solution-like spectra in the single molecule spectra data is taken into account (Figure 4c-1 and 4c-2). Considering a rigid polymer backbone and a limited number of repeat units, the high polarization anisotropy might mean that PBTTT-14 molecules in the SMS sample showing solution-like spectra probably have a rod-like polymer chain with aligned rigid segments connected with a limited number of defects such as σ-bond rotation or imperfect thiophene rings (presence of saturated carbon atoms in thiophene ring).[29−31] This rod-like conformation of PBTTT-14, however, is distinct from the folded conformation observed in PBTTT-14 nanocrystal growth investigation.[8]

PTzQT-12. With regard to PTzQT-12, as can be seen in Figure 4d-1, the emission maximum of the single molecule ensemble spectrum at 600 nm is close to that of its molecular solution at 593 nm. The peak wavelength distribution histogram shown in Figure 4d-2 can be fitted to three Gaussians. Corresponding subensemble emission spectra were constructed and are displayed in Figure 4d-3. The green subensemble spectrum has its emission maximum at 586 nm, which is close to the solution spectrum emission peak at 593 nm. The bimodal distribution for the red-shifted single molecule spectra is again similar to that found in RR-P3HT and indicates the formation of loosely and strongly aggregated conformations. This finding implies that the majority of PTzQT-12 single molecules adopt a molecular solution conformation, whereas ∼35% of the molecules form low energy emission sites.[9] Finally, again the appearance of defined vibronic structure for the magenta and red subensemble spectra is indicative of emission occurring from a limited number of emitters on the chains.[26] As shown in Figure 5d, PTzQT-12 molecules exhibit a somewhat broad P distribution similar to PQT-12. The large number of occurrences of P values of 0.6 and larger suggests that the majority of the polymer chains formed highly ordered structures, even though 65% of the chains exhibit solution-like emission. This indicates that a substantial fraction of the solution-like extended chains form rod-like (highly aligned) morphologies. This observation matches up well the crystal structure analysis by TEM, which revealed that PTzQT-12 chains exhibit nonfolding characteristics.

Comparison of RR-P3HT, PQT-12, PBTTT-14, and PTzQT-12. A summary of the observations made in terms of folding properties of the four polymers studied both in nanocrystals and at single molecule level are listed in Table 1. RR-P3HT exhibits the highest tendency to form collapsed ordered conformations (loosely or strongly aggregated). PQT-12, with a relative rigid polymer backbone due to a higher σ-bond rotation barrier compared with RR-P3HT,[8] displays an absence of emission from strongly aggregated conformations as found in RR-P3HT, which implies a less collapsed (loosely aggregated) conformation in relation to RR-P3HT. Though PBTTT-14 is expected to exhibit a high degree of folding,[8] its SMS data show that half of the molecules retains solution-like spectra and half exhibit aggregate (loosely and strongly) emission. Together with the high P values, these findings are indicative of extended rod-like chain conformations and ordered aggregated chains of PBTTT-14. PTzQT-12, on the basis of observations made for nanocrystals and modeling data, exhibits the most rigid polymer backbone and has ∼65% molecules assuming molecular solution-like spectra and ∼35% with aggregated emission. From the SMS data it thus appears that chain rigidity increases from RR-P3HT to PQT-12, PBTTT-14, and PTzQT-12, with RR-P3HT exhibiting the least chain rigidity and PTzQT-12 exhibiting the most chain rigidity among these four polymers. This only partially agrees with previously reported and current work folding properties in nanowires and nanoribbons, and computational data on σ bond rotation energies. PQT-12 (nonfolding in nanostructures) almost exclusively shows folded chains, PBTTT-14 shows an unexpectedly large occurrence of rod-like chain conformations, and PTzQT-12 (nonfolding in nanostructures) shows a substantial fraction of chains that exhibit loosely or strongly aggregated conformations, albeit to a much lesser extent than PQT-12. The comparison of these results with the folding properties observed in nanocrystals thus clearly illustrates that the folding properties of crystalline conjugated polymers are determined not only by backbone architecture but also by other potential factors such as side chains, intermolecular stacking interactions, and solvent effects during crystal growth.

■ CONCLUSION

The molecular level folding properties of four thiophene-based conjugated polymers including RR-P3HT, PBTTT-14, PTzQT-12, and PQT-12 were studied and correlated to the chemical structure and rigidness of the polymer backbones using single molecule spectroscopy. Analogous to its folding properties in nanostrucutres, it was found that RR-P3HT single chains almost exclusively fold into loosely and strongly aggregated conformations. PQT-12, bearing a similar polymer backbone as RR-P3HT, displays significant chain folding into chains with loosely aggregated conformation but reveals an absence of strongly aggregated polymer chains. The polymer PBTTT-14, compared to RR-P3HT, also exhibits less folding due to a more rigid polymer chain. The findings made for single molecules of PQT-12 and PBTTT-14 are in contrast with the observations made in their corresponding nanostructures where PQT-12 chains exhibit nonfolding properties and PBTTT-14 chains have a strong tendency to fold. PTzQT-12 appears to be the most rigid and planar conjugated polymer of these four polymers. However, although the presumably nonfolding polymers PQT-12 and PTzQT-12 exhibit less folding than RR-P3HT, there is still a significant occurrence of chain folding for these polymers at the single molecule level. The comparison of these results with the folding properties observed in nanocrystals thus clearly illustrate that the folding properties of crystalline conjugated polymers are not only determined by backbone rigidness but also by other factors such as side chains, intermolecular stacking interactions, and solvent effects during crystal growth. These single molecule spectroscopy results provide a single molecule level insight into conjugated polymer chain folding properties as a function of chemical architecture, and are important for understanding macroscale crystallization behavior.

■ AUTHOR INFORMATION

Corresponding Author

*E-mail: A.J.G., andre@ucf.edu; L.Z., lzhai@ucf.edu.

Present Addresses

[†]Center for Nano and Molecular Science and Technology, and Department of Chemistry and Biochemistry, University of Texas at Austin, TX 78712, USA.

[‡]Center for Polymers and Organic Solids, and Department of Chemistry and Biochemistry, University of California at Santa Barbara, CA 93106, USA.

Notes

The authors declare no competing financial interest.

■ ACKNOWLEDGMENTS

The authors gratefully acknowledge the National Science Foundation (NSF) for financial support of this work through a CAREER award (CBET-0746210, A.J.G.), award ECCS-0801924 (A.J.G.), and CAREER award (DMR-0746499, L.Z.). The work is also supported by the Scialog Program from Research Corporation for Science Advancement.

■ REFERENCES

(1) Lim, J. A.; Liu, F.; Ferdous, S.; Muthukumar, M.; Briseno, A. L. *Mater. Today* **2010**, *13* (5), 14−24.

(2) Salleo, A. *Mater. Today* **2007**, *10* (3), 38−45.

(3) Mena-Osteritz, E.; Meyer, A.; Langeveld-Voss, B. M. W.; Janssen, R. A. J.; Meijer, E. W.; Bauerle, P. *Angew. Chem., Int. Ed.* **2000**, *39* (15), 2680−2684.

(4) Brun, M.; Demadrille, R.; Rannou, P.; Pron, A.; Travers, J. P.; Grevin, B. *Adv. Mater.* **2004**, *16* (23−24), 2087−2092.

(5) Payerne, R.; Brun, M.; Rannou, P.; Baptist, R.; Grevin, B. *Synth. Met.* **2004**, *146* (3), 311−315.

(6) Perepichka, I. F.; Perepichka, D. F. *Handbook of thiophene-based materials*; Wiley: Hoboken, 2009.

(7) Liu, J. H.; Arif, M.; Zou, J. H.; Khondaker, S. I.; Zhai, L. *Macromolecules* **2009**, *42* (24), 9390−9393.

(8) Liu, J.; Mikhailov, I. A.; Zou, J.; Osaka, I.; Masunov, A. E.; McCullough, R. D.; Zhai, L. *Polymer* **2011**, *52* (10), 2302−2309.

(9) Barbara, P. F.; Gesquiere, A. J.; Park, S. J.; Lee, Y. J. *Acc. Chem. Res.* **2005**, *38* (7), 602−610.

(10) Hu, Z. J.; Zou, J. H.; Deibel, C.; Gesquiere, A. J.; Zhai, L. *Macromol. Chem. Phys.* **2010**, *211* (22), 2416−2424.

(11) Lupton, J. M. *Adv. Mater.* **2010**, *22* (15), 1689−1721.

(12) Palacios, R. E.; Barbara, P. F. *J. Fluoresc.* **2007**, *17*, 749−757.

(13) Bolinger, J. C.; Traub, M. C.; Brazard, J.; Adachi, T.; Barbara, P. F.; Vanden Bout, D. A. *Acc. Chem. Res.* **2012**, *45*, 1992−2001.

(14) Vogelsang, J.; Brazard, J.; Adachi, T.; Bolinger, J. C.; Barbara, P. F. *Angew. Chem., Int. Ed.* **2011**, *50* (10), 2257−2261.

(15) Vogelsang, J.; Lupton, J. M. *J. Phys. Chem. Lett.* **2012**, *3* (11), 1503−1513.

(16) O'Connor, B.; Chan, E. P.; Chan, C.; Conrad, B. R.; Richter, L. J.; Kline, R. J.; Heeney, M.; McCulloch, I.; Soles, C. L.; DeLongchamp, D. M. *ACS Nano* **2010**, *4* (12), 7538−7544.

(17) Sun, Q. J.; Park, K.; Dai, L. M. *J. Phys. Chem. C* **2009**, *113* (18), 7892−7897.

(18) Wang, S.; Tang, J. C.; Zhao, L. H.; Png, R. Q.; Wong, L. Y.; Chia, P. J.; Chan, H. S. O.; Ho, P. K. H.; Chua, L. L. *Appl. Phys. Lett.* **2008**, *93*, 16.

(19) Cook, S.; Furube, A.; Katoh, R. *Energy Environ Sci.* **2008**, *1* (2), 294−299.

(20) Taliani, C.; Blinov, L. M. *Adv. Mater.* **1996**, *8* (4), 353−359.

(21) Osaka, I.; Sauve, G.; Zhang, R.; Kowalewski, T.; McCullough, R. D. *Adv. Mater.* **2007**, *19* (23), 4160−4165.

(22) Osaka, I.; Zhang, R.; Sauve, G.; Smilgies, D. M.; Kowalewski, T.; McCullough, R. D. *J. Am. Chem. Soc.* **2009**, *131* (7), 2521−2529.

(23) Zhang, X. N.; Johnson, J. P.; Kampf, J. W.; Matzger, A. J. *Chem. Mater.* **2006**, *18* (15), 3470−3476.

(24) Zhang, X. N.; Matzger, A. J. *J. Org. Chem.* **2003**, *68* (25), 9813−9815.

(25) Yu, Z. H.; Barbara, P. F. *J. Phys. Chem. B* **2004**, *108* (31), 11321−11326.

(26) Yu, J.; Hu, D. H.; Barbara, P. F. *Science* **2000**, *289* (5483), 1327−1330.

(27) Quan, S. Y.; Teng, F.; Xu, Z.; Quan, L.; Zhang, T.; Liu, D.; Hou, Y. B.; Wang, Y. S.; Xu, X. R. *J. Lumin.* **2007**, *124* (1), 81−84.

(28) Adachi, T.; Brazard, J.; Ono, R. J.; Hanson, B.; Traub, M. C.; Wu, Z. Q.; Li, Z. C.; Bolinger, J. C.; Ganesan, V.; Bielawski, C. W.; et al. *J. Phys. Chem. Lett.* **2011**, *2* (12), 1400−1404.

(29) Feng, D. Q.; Caruso, A. N.; Losovyj, Y. B.; Shulz, D. L.; Dowben, P. A. *Polym. Eng. Sci.* **2007**, *47*, 1359−1364.

(30) Bugar, I.; Kovac, J.; Matuszna, K.; Lukes, V.; Cik, G. *Laser Phys.* **2004**, *14* (4), 527−532.

(31) Wise, D. L. *Electrical and optical polymer systems*; M. Dekker: New York, 1998; p xii, 1239 pp.

(32) Liu, J. S.; Loewe, R. S.; McCullough, R. D. *Macromolecules* **1999**, *32* (18), 5777−5785.